

# Intrusive gravity currents propagating along thin and thick interfaces

BRUCE R. SUTHERLAND AND JOSHUA T. NAULT

Department of Mathematical and Statistical Sciences, University of Alberta, Edmonton, AB,  
Canada T6G 2G1

(Received 23 March 2007 and in revised form 5 June 2007)

Inviscid gravity currents released from a finite-length lock are known to propagate at a constant speed to a predicted finite distance before decelerating. By extension this should occur in a two-layer fluid with equal upper- and lower-layer depths for an intrusion having the average density of the ambient. The experiments presented here show this is not necessarily the case. The finite-depth thickness of the interface non-negligibly influences the evolution of the intrusion so that it propagates well beyond the predicted constant-speed limit; it propagates without decelerating beyond 22 lock lengths in a rectilinear geometry and beyond 6 lock radii in an axisymmetric geometry. Experiments and numerical simulations demonstrate that the intrusion speed decreases to half the two-layer speed in the circumstance in which the interface spans the domain. The corresponding long mode-2 interfacial wave speed increases rapidly with interfacial thickness, becoming comparable with the intrusion speed when the interfacial thickness is approximately one-quarter the domain height. For somewhat thinner interfacial thicknesses, the intrusion excites solitary waves that move faster than the long-wave speed. The coupling between intrusions and the waves they excite, together with reduced mixing of the current head, result in constant-speed propagation for longer times.

---

## 1. Introduction

Fluid of one density propagating horizontally into an ambient fluid of different density is called a gravity current. These appear in a wide range of circumstances (Simpson 1997) including the spread of oil slicks and river plumes near the ocean surface and the advance of cold air along the ground from a thunderstorm outflow or sea breeze front. Gravity currents can also propagate within an ambient fluid whose density varies with height. These are visible, for example, as rope clouds that propagate radially away from a thunderstorm along the tropopause. Here we call them ‘intrusions’ or ‘intrusive gravity currents’ to distinguish them from gravity currents that move along the upper or lower boundaries of the ambient.

Compared to gravity current research, the dynamics of intrusions are less well understood. Most laboratory experiments have examined vertically symmetric circumstances that are amenable to theoretical analysis. These include intrusions that have density equal to the average ambient density and which propagate in uniformly stratified fluid (Wu 1969; Manins 1976; Amen & Maxworthy 1980) and in a two-layer fluid with equal upper- and lower-layer depths (Britter & Simpson 1981; Faust & Plate 1984; Rooij, Linden & Dalziel 1999; Lowe, Linden & Rottman 2002; Mehta, Sutherland & Kyba 2002). Most studies have neglected the effect of intermediate interfacial thickness upon the evolution of the intrusion, beyond

qualitative experimental observations (Britter & Simpson 1981), and measurements of intrusion speeds travelling less than one lock length (Faust & Plate 1984).

Recent fully nonlinear and shallow-water simulations of gravity currents in uniformly stratified fluid have concluded that stratification and, in particular, the influence of internal waves upon the evolution of the currents is insignificant (Ungarish & Huppert 2006; Huppert 2006). However, at an interface where the stratification is locally strong internal wave speeds are fast and their influence upon the relatively slow moving current is not well understood.

In a long rectangular tank the steady-state speed of an energy-conserving Boussinesq gravity current in an ambient fluid of depth  $h_0$  is predicted to be

$$U_0 = \frac{1}{2}(g'h_0)^{1/2}, \text{ in which } g' = g \frac{|\rho_\ell - \rho_0|}{\rho_{00}}. \quad (1.1)$$

In the definition of the reduced gravity,  $g'$ ,  $\rho_\ell$  is the density of the gravity current,  $\rho_0$  is the density of the ambient fluid and  $\rho_{00}$  is a characteristic density (Benjamin 1968). This definition predicts the speed of both bottom-propagating gravity currents, in which case  $\rho_\ell > \rho_0$ , and surface gravity currents, in which case  $\rho_\ell < \rho_0$ . The same theory predicts that the height of the gravity current spans half the depth of the tank.

It is straightforward to adapt this result to a two-layer fluid. The theoretical steady-state speed of a vertically symmetric intrusion in two-layer fluid is given by (1.1) if the lower-layer depth,  $h_1$ , equals the upper-layer depth,  $h_0$ , and if  $\rho_1 - \rho_\ell = \rho_\ell - \rho_0$ , in which  $\rho_0$  and  $\rho_1$  are the densities of the upper and lower layers, respectively.

Gravity currents in a rectangular channel are known to decelerate after propagating between 6 to 10 lock lengths,  $\ell_0$ . The transition occurs when the finite volume of fluid initially in the lock becomes a significant factor in determining the maximum allowable height of the gravity current head (Huppert & Simpson 1980). Or, in another perspective, it occurs when the return flow of the ambient about the gravity current head reflects off the endwall of the lock and the resulting 'rear-bore' catches up with the gravity current head (Rottman & Simpson 1983). By symmetry, these dynamics should also occur for corresponding vertically symmetric intrusions, but experiments have shown that they maintain a constant speed well beyond 10 lock lengths (Mehta *et al.* 2002; Sutherland, Kyba & Flynn 2004*b*).

Although vertically symmetric intrusions in a two-layer fluid do not excite interfacial waves, they may excite internal solitary waves in a three-layer fluid (Mehta *et al.* 2002) and by the collapse of a symmetric, thick-interface, two-layer fluid into another symmetric two-layer fluid with smaller interfacial thickness (Maxworthy 1980). The mechanism for wave generation in these circumstances is in part a symmetric extension of experiments by Kao, Pan & Renouard (1985) who launched solitary waves into a two-layer fluid by releasing a deep layer of fluid into a shallow layer having the same density, and by Grue *et al.* (2000) who launched solitary waves into a thin stratified layer. In some circumstances the solitary waves developed closed cores, meaning that they transported mass long distances along with the wave. In this sense closed-core solitary waves act like gravity currents with the difference that the density of the ambient ahead of a gravity current nowhere matches the density of the current itself (see, for example, figure 1 of Sutherland 2002).

The ambient ahead of intrusions has an isopycnal surface with the same density as the intrusion itself. Thus, there is a fine line between the description of intrusions as gravity currents or as closed-core solitary waves. A solitary wave description would be more appropriate if the interface ahead of the intrusion is thick, in which case there is a relatively deep layer of ambient fluid that closely matches the intrusion

density. The question remains: how thick should this layer be before the intrusion behaves more like a closed-core solitary wave than a gravity current?

These notions may be extended to a circular geometry. Gravity currents released from a cylinder of radius  $r_0$  are observed to decelerate after propagating 1 to 3 lock radii (Huq 1996; Hallworth *et al.* 1996). Even ignoring interactions with a rear bore, the deceleration is expected because, by conservation of mass, the head height must decrease as the current spreads radially and its azimuthal extent increases (Huppert & Simpson 1980). However, as the experiments presented here show, vertically symmetric intrusions released from a cylinder in a two-layer fluid propagate at constant speed well beyond 3 lock radii.

The purpose of this work is to characterize the speed of vertically symmetric intrusions a function of interfacial thickness and to demonstrate by way of experiments and simulations that the transition to long-distance constant propagation speeds occurs when the thickness of the interface is sufficiently large that mode-2 interfacial wave speeds are comparable with the intrusion speed.

## 2. Laboratory experiments

Experiments were performed in three different tanks, most setups being established to examine intrusions propagating at mid-depth in a two-layer fluid with finite interfacial thickness between equal-depth upper and lower layers. One set of experiments studied the effect of interfacial thickness upon intrusions propagating in a long, rectangular tank. Other experiments examined radially propagating flows in which intrusions were released either from a cylinder at the centre of a cylindrical tank or from a quarter-cylinder at the corner of a square tank.

### 2.1. Rectilinear intrusions

Three sets of experiments were performed in a 197.1 cm long, 17.4 cm wide and 48.5 cm tall glass tank. In one set the tank was filled to a depth  $h_0$  with salt water of density  $\rho_1$  and then fresh water of density  $\rho_0$  was carefully poured through a sponge float until the total fluid depth was  $2h_0$ . By covering the tank to inhibit surface evaporation and letting the system rest for a long period of time, the interface between the two fluids diffusively broadened. The resulting density profile was measured with a vertically traversing conductivity probe (Precision Measurement Engineering). The half-thickness of the interface was estimated by

$$h_\rho \equiv \frac{1}{2} \frac{\rho_1 - \rho_0}{|d\bar{\rho}/dz|_{z=h_0}}. \quad (2.1)$$

In another set of intrusion experiments, the tank was filled with uniformly salt-stratified fluid using the standard ‘double-bucket’ technique. Again, the density gradient was measured using the conductivity probe to confirm that the density gradient was constant from the top to bottom of the tank. For these experiments we define  $h_\rho = h_0$ .

In surface-propagating gravity current experiments the tank was filled to a depth  $h_0 - h_\rho$  with salt water and a thin layer of fresh water with depth  $h_\rho$  was layered on top. The fluid was allowed to diffuse so the density gradient near the surface was approximately linear.

In all three sets of experiments, after filling and waiting, a gate was inserted vertically between a pair of glass inserts thus forming a lock of length  $\ell_0$  near the left-end of the tank. In intrusion experiments the fluid in the lock was thoroughly

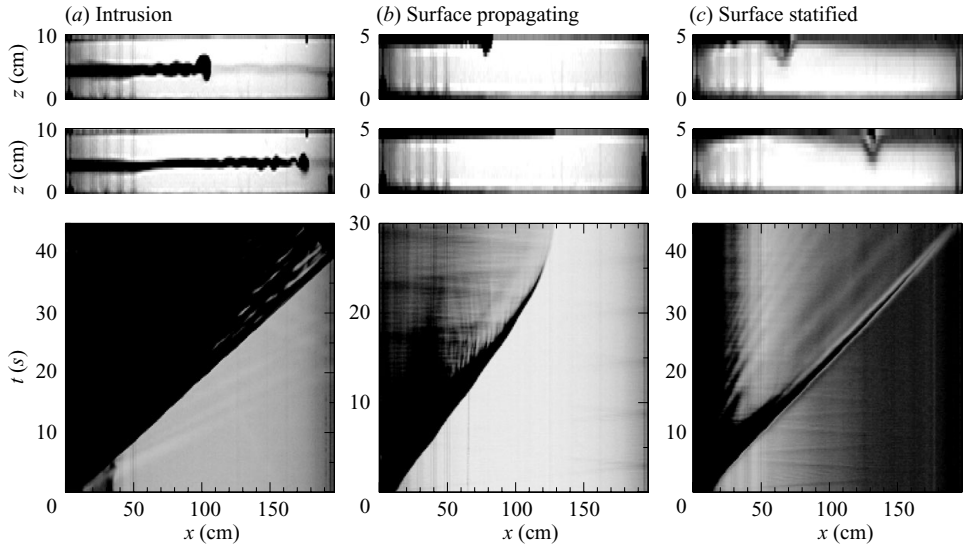


FIGURE 1. (a) The top two images show side views of an intrusion experiment at times  $t \simeq 20$  s and 35 s, respectively, and the bottom image shows the corresponding horizontal time series constructed from slices taken through movies at  $z = h_0$ . In this experiment  $h_0 = 5$  cm,  $\rho_\ell - \rho_0 = 0.026$  g cm $^{-3}$ ,  $\ell_0 = 8.5$  cm and  $\delta_h = 0.10$ . (b) As (a) but for a surface-propagating gravity current experiment with  $h_0 = 5$  cm,  $|\rho_\ell - \rho_0| = 0.027$  g cm $^{-3}$ ,  $\ell_0 = 8.5$  cm and  $\delta_h = 0$ . (Note the different time axis.) (c) As (a) but for a surface-propagating gravity current experiment with  $h_0 = 5$  cm,  $|\rho_\ell - \rho_0| = 0.027$  g cm $^{-3}$ ,  $\ell_0 = 8.5$  cm and  $\delta_h = 0.26$ .

mixed so that the lock-fluid had density,  $\rho_\ell$ , equal to the average density of the ambient and, by symmetry, equal to the density of the ambient fluid at mid-depth in the tank. In surface-propagating gravity current experiments, the lock fluid was replaced with fresh water. In typical experiments  $h_0 = 5$  cm,  $\ell_0 = 8.5$  cm and  $|\rho_\ell - \rho_0| \simeq 0.025$  g cm $^{-3}$ .

To visualize the motion of the intrusion, food colouring was mixed into the lock fluid. The volume of dye was sufficiently small (approximately 1 ml) that it did not significantly change the density of the lock fluid.

The experiment proceeded by rapidly extracting the gate and recording the along-tank motion of the intrusion by a digital video camera situated 3.5 m in front of the tank. Time series were constructed from a sequence of horizontal slices taken at the depth  $z = h_0$ , and from these the position of the intrusion front as a function of time could be established.

The main non-dimensional parameter governing the experiments was

$$\delta_h = \frac{h_\rho}{h_0}, \quad (2.2)$$

which measures the ratio of the half-depth of the interface to the half-depth of the tank.

Two other non-dimensional parameters were  $\delta_\ell = \ell_0/h_0$  and  $\delta_\rho = |\rho_\ell - \rho_0|/\rho_0$ . The former inconsequentially affected the intrusion speed provided it was sufficiently large. The intrusion speed was found to vary as the square root of  $\delta_\rho$  as expected from (1.1). The Reynolds number based on  $U_0$  and  $h_0$  ranged from 1000 to 20000. These values were sufficiently large that viscous diffusion negligibly affected the intrusion speed.

The results of three experiments are shown in figure 1. The horizontal time series taken from the intrusion experiment (figure 1a) shows that the intrusion propagates

at constant speed to the end of the tank, a distance of 22.2 lock lengths. During its progress the intrusion head became smaller and trailing interfacial waves were apparent, though the interface ahead of the intrusion was effectively motionless.

By contrast, figure 1(b) shows that a fresh water current propagating along the surface of an ambient of uniform-density salt water decelerates after propagating approximately 10 lock lengths. This is consistent with theory, although the deceleration can be attributed as much to significant mixing of the current head as to a rear bore that catches up to the current head. At 35 s, the current became wedge-shaped and stopped propagating.

If the near surface of the ambient is stratified over sufficient depth, a surface-propagating current maintains a head as it propagates at constant speed to the end of the tank (figure 1c). Movies show that there is less mixing of the head, presumably because the density gradient and shear between the head and ambient decrease such that the local Richardson number is larger. This relationship between density gradient and shear has also been noted in tilting-tank experiments (Thorpe 1968).

Disturbances to a thin dye layer near the top of the tank reveal the generation of a solitary internal wave which encloses the gravity-current head. The current and wave speed are identical. Other experiments (not shown) reveal that the wave continues to propagate at constant speed after the lock fluid, having travelled sufficiently far from the gate, is depleted.

Although only three experiments have been shown here, we have found that the intrusion speed is constant well beyond 10 lock lengths for a range of experiments with  $\delta_h$  ranging from 0.08 to 1,  $\delta_\rho$  ranging from 0.002 to 0.055 and  $\delta_\ell$  ranging from 0.43 to 1.7.

## 2.2. Radially spreading intrusions

Unlike gravity currents released in a rectangular tank, radially spreading currents decrease in height over time soon after their release, in part as a consequence of azimuthal spreading. Thus the horizontal pressure gradient between the current and ambient must decrease and the flow decelerates after propagating a distance on the order of the lock radius. This should also occur for a vertically symmetric intrusion in a two-layer fluid. We have seen, however, that rectilinear intrusions propagate at constant speed even though their head height evolves to be comparable with the interfacial thickness. It turns out that this result extends to radially spreading intrusions.

Most experiments were performed in a 30.0 cm high cylindrical acrylic tank having an inner diameter of 90.7 cm. The ambient fluid was established as in the rectilinear tank, except that experiments were performed shortly after filling the tank so that in two-layer experiments the interface did not diffusively broaden by much beyond the thickness established due to mixing during the filling stage. Typically the interface half-thickness was  $h_\rho \simeq 0.5$  cm.

An acrylic cylinder of inner radius  $r_0$  was inserted at the centre of the tank and the fluid inside was dyed and thoroughly mixed. A set of strings attached to the top of the cylinder passed through a pulley situated well above the tank and returned to the level of the tank. Thus, by pulling on the strings, the cylinder was extracted nearly vertically. This process was deemed successful if the resulting intrusion spread radially at equal rates in all directions. In most experiments,  $r_0 = 6.0$  cm and  $h_0 = 5$  cm. Typically,  $\delta_h = 0.1$  and  $\delta_\rho$  ranged between 0.055 and 0.142.

The tank was placed beneath a frame supporting a COHU CCD camera situated 2 m above the centre of the tank. A grid of radial lines (spaced by 90°) and concentric

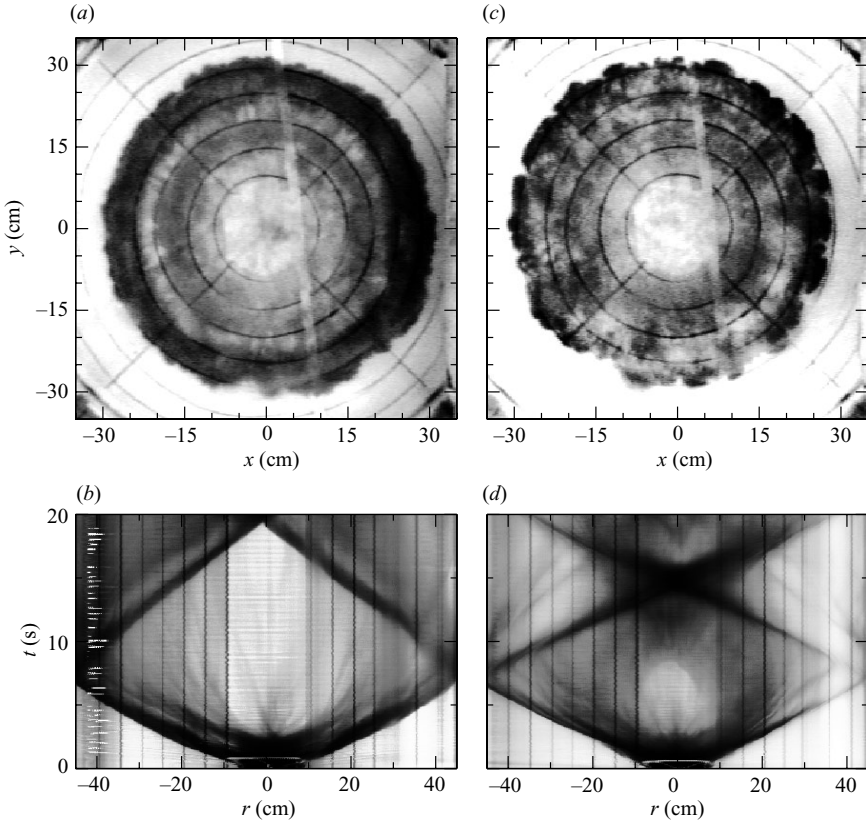


FIGURE 2. (a) Top view taken 4.5 s after lock release for a bottom-propagating gravity current released from a cylinder at the centre of a cylindrical tank, and (b) corresponding time series taken along the diameter of the tank. Darker regions of dye indicate where the head height is thicker. Here  $h_0 = 10$  cm and  $\rho_\ell - \rho_0 = 0.0533$  g cm $^{-3}$ . (c, d) As (a, b) but for an intrusive gravity current experiment with  $h_0 = 5$  cm,  $h_1 = h_0$ , and  $\rho_\ell - \rho_0 = \rho_1 - \rho_\ell = 0.0533$  g cm $^{-3}$ .

circles (spaced by 5 cm) were drawn on the bottom of the tank to help establish actual coordinates from images of the experiments. Time-series plots were constructed from slices across a diameter of top-view images taken by the camera. These were used to measure the intrusion and gravity current positions over time.

For comparison, a snapshot and time series image of a control experiment consisting of an axisymmetric bottom-propagating gravity current are shown in figure 2(a). Corresponding images of a vertically symmetric, radially spreading intrusion are shown in figure 2(b).

As is well documented (Didden & Maxworthy 1982) the bottom-propagating gravity current propagates with a well-defined head (figure 2a) and decelerates as it moves outward (figure 2b). In comparison, the intrusion head shown in figure 2(c) is not so well-defined. The structure of the front is more corrugated and the radial extent of the lee of the head is not easily identified. This change in structure cannot be identified with a lobe-and-cleft instability, which results from the no-slip condition felt by bottom-propagating gravity currents. Instead it appears to be caused by an instability resulting from the interaction of the radially spreading intrusion with the stratified interface. Despite the breakdown of the azimuthally symmetric structure, the front is observed to advance at constant speed to the radius of the tank, a distance of

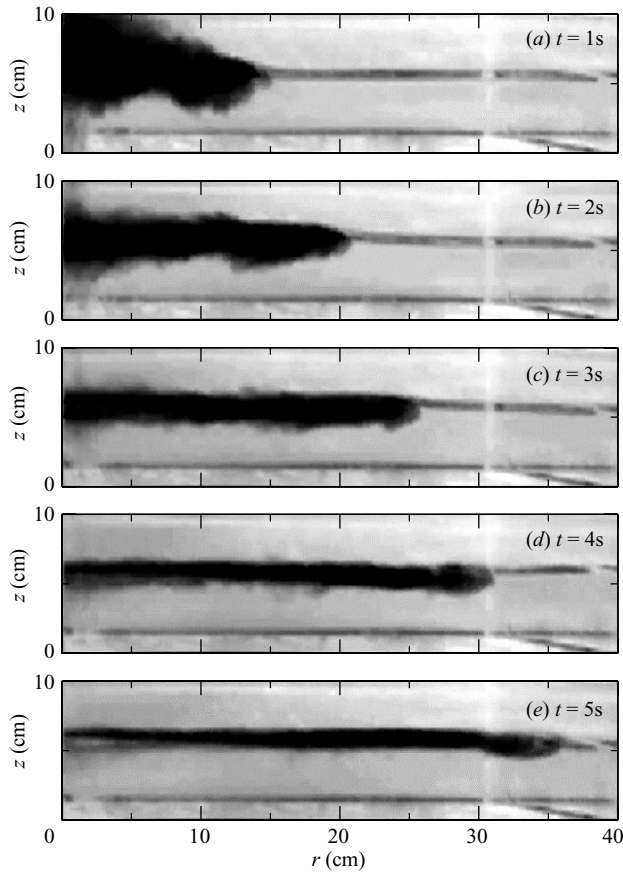


FIGURE 3. Successive snapshots of a vertically symmetric intrusive gravity current spreading radially from the corner of a square tank.

6.6 lock radii, and it continues to propagate inward at constant speed upon reflection from the tank sidewalls. Because the intrusion advances along ‘spokes’ the head height does not necessarily decrease as it must if it spread uniformly azimuthally.

An effective cross-section side view of the intrusion experiment is established through experiments that were performed in a square acrylic 40 cm tall tank measuring 40 cm by 40 cm in the horizontal. The intrusion was released from a quarter-cylinder of radius 5.5 cm in one corner of the tank and a camera recorded the advance of the intrusion along the wall of the tank with the cylinder on the left-hand side.

Successive snapshots of this experiment are shown in figure 3. These demonstrate that the intrusion structure was elongated with no clear bulbous head and that the head height decreased as it advanced radially. Horizontal time series (not shown) confirmed that the propagation speed was constant from one end of the tank to the other.

### 3. Numerical simulations

The experiments have shown that intrusions at a finite-depth interface propagate at constant speed even when the head height decreases. Our intention here is to simulate the evolution of the intrusions to examine how their speed varies with the structure

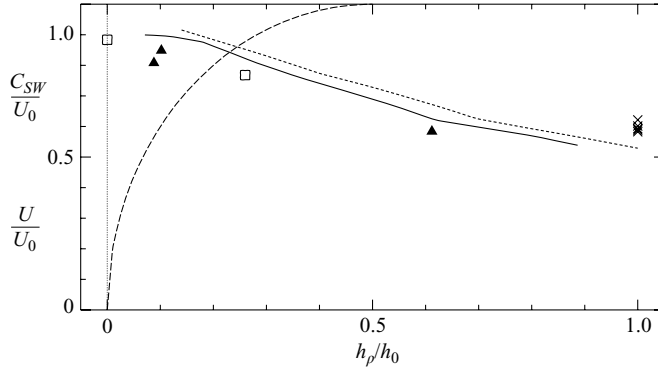


FIGURE 4. Experimentally measured and simulated normalized intrusion speeds,  $U/U_0$  plotted as a function of normalized interfacial thickness,  $\delta_h$ . Experiments: surface-propagating currents ( $\square$ ), intrusions at thick interfaces ( $\blacktriangle$ ) and intrusions in uniformly stratified fluid ( $\times$ ). The lines represent simulated speeds of intrusions in an ambient density profile in the form of an error function (solid line) and piecewise-linear curve (dotted line). The dashed line plots  $C_{SW}/U_0$ , the ratio of the shallow water wave speed to  $U_0$ .

and thickness of the interface as well as to compare the speed with interfacial wave speeds.

The propagation of intrusions and surface currents in a rectilinear geometry is simulated using a code that solves the fully nonlinear Boussinesq equations of motion for vorticity and density, as described by Sutherland, Flynn & Dohan (2004a). Although restricted to two dimensions, simulations run with experimental parameters (not shown) demonstrate that the speed and structure of the intrusions are captured well. In particular, intrusions are found to propagate at constant speed to the end of the tank whereas gravity currents on a free-slip surface are found to decelerate after propagating approximately 10 lock lengths.

In high-resolution simulations designed to measure the speed of intrusions, the total height of the domain was set to unity, the simulated lock length was  $\ell_0 = 2h_0 = 1$  and the horizontal extent of the domain was  $5\ell_0$ . The ambient density profile was prescribed either as an error-function or as a piecewise-linear profile with  $\rho$  decreasing linearly from  $\rho_1$  to  $\rho_0$  at mid-depth over a distance  $2h_\rho$ . In either case, the depth,  $h_\rho$ , of the interface is prescribed by (2.1). The vertical resolution,  $\Delta z$ , was set so that  $\Delta z/h_0 < 0.002$  in all simulations.

At each time step, the computed velocity fields were used to advect a passive tracer field which initially was set to have a concentration of unity over the domain of the lock and zero elsewhere. Horizontal time series extracted from slices at mid-depth through snapshots of the passive tracer field were then used to determine the speed of the simulated intrusions.

The results of experiments and simulations are shown in figure 4. Generally we find that as  $\delta_h$  increases to unity, the intrusion speed decreases monotonically to about 50% of the speed of an intrusion at an infinitesimally thin interface. The speed is relatively insensitive to the structure of the interface as indicated by the comparable speeds for intrusions propagating in an ambient with an error-function and a piecewise-linear density profile.

The experimentally measured intrusion speeds are somewhat less than the simulated speeds if  $\delta_h < 1$ . In particular, the surface-propagating current in a uniform ambient (for which  $\delta_h = 0$ ) moves approximately 10% slower than the predicted speed. This is



attributed to the small lock length used in the experiments; when the gate is extracted turbulence resulting from its extraction non-negligibly affects mixing between the ambient and lock fluid.

#### 4. Discussion and conclusions

Laboratory experiments and numerical simulations show that intrusion speeds decrease monotonically from  $U_0$ , the two-layer theory prediction, to approximately  $0.5U_0$  as the relative interfacial thickness  $\delta_h$  increases from 0 toward unity. In experiments with a diffuse interface (having an error-function density profile), as  $\delta_h \rightarrow 1$  the density difference between the top and bottom of the domain decreases non-negligibly and thus affects the intrusion speed. The experimentally measured normalized speed of the intrusion in uniformly stratified fluid (with a linear density profile) is approximately the same as the intrusion speed along a diffuse interface with  $\delta_h \simeq 0.6$ . Although simulations exhibit a monotonic decrease in speed with increasing  $\delta_h$ , the speed observed in experiments levels off, perhaps due to mixing associated with the gate removal.

For small but finite interfacial thicknesses, rectilinear intrusions are observed to propagate much further than 10 lock lengths and, likewise, axisymmetric intrusions propagate well beyond 3 lock radii at constant speed. Numerical simulations of rectilinear intrusions show that this effect can be captured in a model that restricts the dynamics to two dimensions and which neglects mixing resulting from extraction of the gate from the lock. The long-time steady-state propagation phase is a consequence of the finite-depth interfacial thickness.

Figure 4 gives insight into the physical processes that govern this transition from short- to long-time steady-state behaviour as a function of interfacial thickness. The dashed line plots for  $0 \leq \delta_h \leq 0.5$  the long interfacial wave speed  $C_{sw} = \sqrt{g'\bar{h}}$ , in which  $\bar{h} = h_0\delta_h(1 - \delta_h)$ , normalized with  $U_0$ . This assumes the interface has uniform density  $\rho_\ell$  over a depth  $h_\rho$  and, correspondingly,  $g'$  is given by (1.1). For  $C_{sw}/U_0$  as small as 0.15, the interfacial wave speed is comparable to the intrusion speed.

The surface-propagating gravity current experiments in which the surface is stratified (figure 1c) show that the flow excites a solitary wave, which is known to propagate faster than the shallow-water wave speed (Whitham 1974). Once launched, the wave rather than the current dictates the evolution: the motion is better described as a 'leaky' closed-core solitary wave, which loses fluid associated with the initial intrusion to the trailing flow behind the wave. Although the generation of the wave may negligibly affect the initial intrusion speed (Flynn & Linden 2006), it does play an important role in transferring mass and energy long distances at constant speed. Apparently this is also the case in an axisymmetric geometry, in which case radially spreading waves transport mass long distances at constant speed even when their amplitude necessarily decreases.

The main point of this research is to demonstrate the applicability and limitations of applying two-layer theory to intrusions. In reality, geophysical interfaces do not have infinitesimally thin interfaces. Although the propagation of interfacial waves depends weakly upon interfacial thickness, the interaction between intrusions and waves cannot be neglected except in special circumstances.

We are grateful for the comments of the referees which have helped to clarify points raised in this paper. This research was supported by the Canadian Foundation for Climate and Atmospheric Science (CFCAS).

## REFERENCES

- AMEN, R. & MAXWORTHY, T. 1980 The gravitational collapse of a mixed region into a linearly stratified solution. *J. Fluid Mech.* **96**, 65–80.
- BENJAMIN, T. B. 1968 Gravity currents and related phenomena. *J. Fluid Mech.* **31**, 209–248.
- BRITTER, R. E. & SIMPSON, J. E. 1981 A note on the structure of the head of an intrusive gravity current. *J. Fluid Mech.* **112**, 459–466.
- DIDDEN, N. & MAXWORTHY, T. 1982 The viscous spreading of plane and axisymmetric gravity currents. *J. Fluid Mech.* **121**, 27–42.
- FAUST, K. M. & PLATE, E. J. 1984 Experimental investigation of intrusive gravity currents entering stably stratified fluids. *J. Hydraul. Res.* **22** (5), 315–325.
- FLYNN, M. R. & LINDEN, P. F. 2006 Intrusive gravity currents. *J. Fluid Mech.* **568**, 193–2002.
- GRUE, J., JENSEN, A., RUSOAS, P.-O. & SVEEN, J. K. 2000 Breaking and broadening of internal solitary waves. *J. Fluid Mech.* **413**, 181–217.
- HALLWORTH, M. A., HUPPERT, H. E., PHILLIPS, J. C. & SPARKS, R. S. J. 1996 Entrainment into two-dimensional and axisymmetric turbulent gravity currents. *J. Fluid Mech.* **308**, 289–311.
- HUPPERT, H. E. 2006 Gravity currents: a personal perspective. *J. Fluid Mech.* **554**, 299–322.
- HUPPERT, H. E. & SIMPSON, J. E. 1980 The slumping of gravity currents. *J. Fluid Mech.* **99**, 785–799.
- HUQ, P. 1996 The role of aspect ratio on entrainment rates of instantaneous, axisymmetric finite volume releases of dense fluid. *J. Hazardous Mater.* **49**, 89–101.
- KAO, T. W., PAN, F.-S. & RENOARD, D. 1985 Internal solitons on the pycnocline: Generation, propagation, and shoaling and breaking over a slope. *J. Fluid Mech.* **159**, 19–53.
- LOWE, R. J., LINDEN, P. F. & ROTTMAN, J. W. 2002 A laboratory study of the velocity structure in an intrusive gravity current. *J. Fluid Mech.* **456**, 33–48.
- MANINS, P. 1976 Intrusion into a stratified media. *J. Fluid Mech.* **74**, 547–560.
- MAXWORTHY, T. 1980 On the formation of nonlinear internal waves from the gravitational collapse of mixed regions in two and three dimensions. *J. Fluid Mech.* **96**, 47–64.
- MEHTA, A., SUTHERLAND, B. R. & KYBA, P. J. 2002 Interfacial gravity currents: Part II – wave excitation. *Phys. Fluids* **14**, 3558–3569.
- ROOIJ, F., LINDEN, P. F. & DALZIEL, S. B. 1999 Saline and particle-driven interfacial intrusions. *J. Fluid Mech.* **389**, 303–334.
- ROTTMAN, J. W. & SIMPSON, J. E. 1983 Gravity currents produced by instantaneous releases of a heavy fluid in a rectangular channel. *J. Fluid Mech.* **135**, 95–110.
- SIMPSON, J. E. 1997 *Gravity Currents*, 2nd edn. Cambridge University Press.
- SUTHERLAND, B. R. 2002 Interfacial gravity currents. I. Mixing and entrainment. *Phys. Fluids* **14**, 2244–2254.
- SUTHERLAND, B. R., FLYNN, M. R. & DOHAN, K. 2004a Internal wave excitation from a collapsing mixed region. *Deep-Sea Res. II* **51**, 2889–2904.
- SUTHERLAND, B. R., KYBA, P. J. & FLYNN, M. R. 2004b Interfacial gravity currents in two-layer fluids. *J. Fluid Mech.* **514**, 327–353.
- THORPE, S. A. 1968 A method of producing a shear flow in a stratified fluid. *J. Fluid Mech.* **32**, 693–704.
- UNGARISH, M. & HUPPERT, H. E. 2006 Energy balances for propagating gravity currents: Homogeneous and stratified ambients. *J. Fluid Mech.* **565**, 363–380.
- WHITHAM, G. B. 1974 *Linear and Nonlinear Waves*. John Wiley and Sons.
- WU, J. 1969 Mixed region collapse with internal wave generation in a density stratified medium. *J. Fluid Mech.* **35**, 531–544.